Analytica Chimica Acta 719 (2012) 43–51

Contents lists available at SciVerse ScienceDirect

Analytica Chimica Acta

journal homepage: www.elsevier.com/locate/aca

Application of multi-way analysis to UV–visible spectroscopy, gas chromatography and electronic nose data for wine ageing evaluation

N. Prieto[a,b], M.L. Rodriguez-Méndez[b], R. Leardi[c], P. Oliveri[c,*], D. Hernando-Esquisabel[d], M. Iñiguez-Crespo[d], J.A. de Saja[a]

[a] Department of Condensed Matter Physics, Faculty of Sciences, University of Valladolid, 47011 Valladolid, Spain
[b] Department of Inorganic Chemistry, Escuela de Ingenierías Industriales, University of Valladolid, Paseo del Cauce, 59, 47011 Valladolid, Spain
[c] Department of Pharmaceutical and Food Chemistry and Technology, University of Genoa, Via Brigata Salerno 13, I-16147 8 Genoa, Italy
[d] Gobierno de la Rioja, Consejería de Agricultura y Alimentación, Estación Enológica, Bretón de los Herreros 4, 26200 Haro, La Rioja, Spain

ARTICLE INFO

Article history:
Received 3 September 2011
Received in revised form
19 December 2011
Accepted 5 January 2012
Available online 12 January 2012

Keywords:
Chemometrics
Multi-way data analysis
Tucker3
Wine ageing
Electronic nose

ABSTRACT

In this study, a multi-way method (Tucker3) was applied to evaluate the performance of an electronic nose for following the ageing of red wines. The odour evaluation carried out with the electronic nose was combined with the quantitative analysis of volatile composition performed by GC–MS, and colour characterisation by UV–visible spectroscopy. Thanks to Tucker3, it was possible to understand connections among data obtained from these three different systems and to estimate the effect of different sources of variability on wine evaluation. In particular, the application of Tucker3 supplied a global visualisation of data structure, which was very informative to understand relationships between sensors responses and chemical composition of wines. The results obtained indicate that the analytical methods employed are useful tools to follow the wine ageing process, to differentiate wine samples according to ageing type (either in barrel or in stainless steel tanks with the addition of small oak wood pieces) and to the origin (French or American) of the oak wood. Finally, it was possible to designate the volatile compounds which play a major role in such a characterisation.

1. Introduction

Alternative techniques for wine ageing process are being increasingly employed in oenology, in order to achieve more pronounced sensory characteristics in products [1]. This practise involves storing wine in stainless steel tanks with oak wood pieces and dosing it with appropriate oxygen quantities in order to obtain a product more stable in time and with the same characteristics of barrel-aged wines [2]. Several studies have investigated the differences between the types of wine ageing, both at chemical and at sensory level [3]. The oak wood provides flavour and aromatic support to the wine, while adding richer, fuller impressions and complexity. Alternative ageing techniques do not represent a replacement for traditional wine ageing in barrels. Anyway, in conjunction with micro-oxygenation (MOX), they allow to produce wines with organoleptic features very similar to wines traditionally aged. However, as there are no general rules about wine-making with alternative techniques, the research in this field is aimed at better understanding the mechanisms of wine evolution during ageing and the particular role that a specific set of conditions plays in the ageing process.

Over the last few years, the development of instruments as electronic noses, able to detect and characterise volatile compounds, have been well reported [4–6]. One of the most interesting characteristics of these systems is the possibility to analyse samples without heavy pretreatments, also in the case of wines, which are very complex matrices. Moreover, using chemometric tools, a description of the sensory characteristics may be obtained. Complementary information may be provided by means of data fusion with methods such as the colour and chromatographic evaluation.

The data set of the present study is a typical 3-way (or 3-mode) array, with the three modes being process types, variables and times.

Tucker3 is one of the most popular N-way methods [7,8], and it can be fairly considered as a natural extension of classical bilinear Principal Component Analysis (PCA). Multi-way methods have been applied to the analysis of different types of instrumental data, mainly spectroscopic ones [9,10]. On the other hand, few applications on GC data have been reported and even fewer works can be referenced in the field of the electronic noses [11,12]. These studies were aimed at evaluating sensory properties of food products [13], obtaining an overview of the characteristics of the volatile fraction for different types of vinegar [14], identifying the correspondence

* Corresponding author. Tel.: +39 010 3532374; fax: +39 010 3532684.
E-mail address: oliveri@dictfa.unige.it (P. Oliveri).

0003-2670/$ – see front matter © 2012 Elsevier B.V. All rights reserved.
doi:10.1016/j.aca.2012.01.009

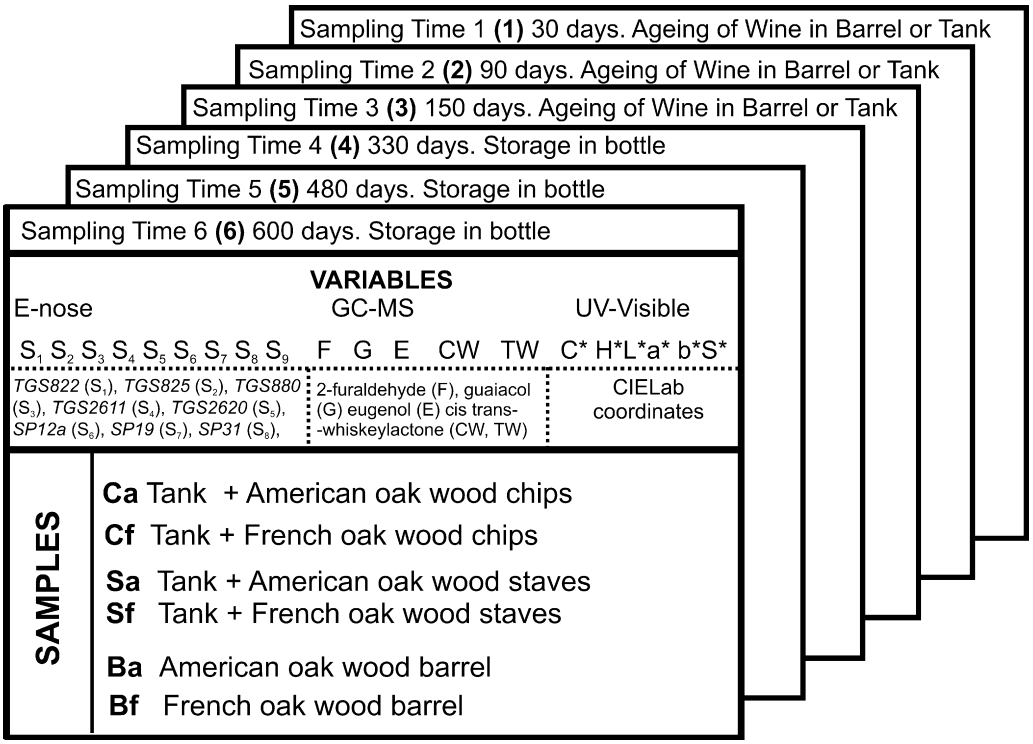

Fig. 1. Graphical representation of the three-way data array.

between attributes and judges for white bread evaluation [7] and discriminating between different olive oils using an MS-based electronic nose e-MS [15].

The aim of the present study was to apply a tool for modelling data obtained from an electronic nose, which were fused to those obtained by classical analytical techniques. Wine samples prepared under different conditions were analysed by means of UV–visible spectroscopy (UV–vis), gas chromatography–mass spectrometry (GC–MS), and a sensor-based electronic nose. Results from spectroscopy were evaluated using the method CIELab according to the protocol established by the OIV [16]. In the case for GC–MS measurements, five volatile compounds which have been reported as key markers throughout wine ageing (2-furaldehyde, guaiacol, *cis*- and *trans*-whiskeylactone and eugenol) have also been evaluated in this work [17]. Finally, the maximum change in the resistance of nine different MOX sensor responses was measured, in order to monitor the volatile organic compounds at different steps of winemaking.

The evaluation was conducted over a period of twenty months; during the first eight months, the wines were kept in barrels or in stainless steel tanks inoculated with oak wood. This work produced a considerable data set derived from six periodical determinations of 20 variables on six different wines. The Tucker3 method allowed: (i) to follow the changes of the volatile organic fraction during the wine ageing process; (ii) to obtain an overview of the differences between the wine aged in barrels or with alternative systems and, finally, (iii) to assess the relationships among the variables measured.

2. Experimental

2.1. Wine samples

The variables studied, the sampling schedule and the winemaking process conditions are described in Fig. 1. Grapes of the variety Tempranillo coming from the D.O. Ribera del Duero (Spain) were involved in the study. After fermentation, the wine obtained was submitted to ageing following different methodologies. One part was prepared by maturing the wine in 100 L stainless steel tanks, in which pieces of oak wood were added: four wines were obtained by adding wood samples of different sizes (chips or staves) and of two different origins (American and French). Two more samples were obtained by ageing the wine in oak barrels (225 L capacity) using American and French oak wood.

In order to assure a comparable surface of wood to be in contact with wine (both in barrels and tanks with pieces of wood added), the surface/volume ratio for the 225 L barrels – whose surface was 2.04 m^2 – was calculated, obtaining a value of 0.0091 $m^2\ L^{-1}$. Thus, 600 g of chips were added to each tank to obtain a similar surface/volume ratio for wood therein. Similar calculations were carried out for staves. In order to monitor their ageing, the six wines under study were analysed periodically: after one month (T1), three months (T2), five months (T3). After eight months, wines aged by different methods were bottled. Further analyses took place at 11 months (T4), 16 months (T5) and 20 months (T6).

2.2. Analysis of colour

Colour measurements were made with a Shimadzu 2101 UV-Vis Spectrophotometer, using a 1 mm path length glass cell [18]. The CIELab coordinates (L*, a*, b*, C, H, S) were calculated following the recommendations of the *Comission Internationale of L'Eclairage* for the CIE illuminant D65 and 10° standard observer conditions.

2.3. Electronic nose

The array of nine gas sensors was constructed using the inorganic metal oxide MOX *TGS822* (S1), *TGS825* (S2), *TGS880* (S3), *TGS2611* (S4), *TGS2620* (S5), *SP12a* (S6), *SP19* (S7), *SP31* (S8), *SPMW1* (S9) sensing units that were selected according to previous studies [19]. Sensors were mounted in a stainless steel test box with an internal volume of 75 mL. The test box was kept at a constant

temperature (50 °C ± 2) during the experiments. Data collection was performed through a PC-LPM-16 data acquisition card from National Instruments, interfaced to a personal computer. Sensors were polarised using a constant voltage of 5 V provided by a FAC-662B programmable power supply. The resistance measurement was taken every 0.5 s. Data were monitored in real time and the graphs could be followed using Visual Basic software from Microsoft.

The solid phase microextraction (SPME) method was used for extracting analytes from samples. A volume of 3 mL of wine was placed in a 10 mL vial that was kept at 40 °C during 15 min, with 650 rpm agitation. Then a bipolar fibre of polydimethylsiloxane coated with carbowax and divinylbenzene (PDMS/CW/DVB, Supelco) was exposed to the headspace of the vial for 15 min. Then, the SPME fibre was placed in the heated injection port of the gas chromatograph at 250 °C. The volatile compounds were driven to the test chamber using a constant gas flow of 150 mL min^{-1} (air 100 mL min^{-1}, nitrogen 50 mL min^{-1}). All wine samples were measured seven times with the electronic nose. The experimental variability was smaller than the differences among samples.

2.4. Gas chromatography

The chromatographic analyses were performed with a Clarus 500 GC equipped with a mass detector Clarus 560 Perkin Elmer, in the splitless mode. A carbowax (length: 30 m; inner diameter: 0.25 mm; film thickness: 0.25 μm) column was used. The temperature programme was: an initial temperature of 40 °C (held constant for 3 min) raised to 80 °C at a rate of 2 °C min^{-1} and held constant for 15 min. Then the temperature was increased at a rate of 3 °C min^{-1} up to 180 °C and held constant for 15 min. The final ramp consisted of increasing the temperature up to 210 °C at a rate of 3 °C min^{-1} and held constant for 5 min.

Volatile compounds were identified using the NIST library, while quantification was performed from the calibration curves of the respective standards in a solution prepared at different concentrations levels. The oak volatile compounds added to the solution (12%, v/v absolute ethanol) were: 2-furaldehyde (F) (Fluka, purity grade >98%), guaiacol (G) (Fluka, purity grade >98%), eugenol (E) (Riedel de Haën, purity grade >99.3%), *cis*-, *trans*-whiskeylactone (CW, TW) (SAFC, purity grade >98%).

2.5. Data processing: Tucker3

Since the same analyses have been performed on the different wines on different times, the real structure of the data set is a three-way array, which can be imagined as a parallelepiped of size $I \times J \times K$, where I is the number of wines (objects), J is the number of variables and K is the number of sampling times (conditions).

To apply standard PCA, these three-way data arrays $\underline{\mathbf{X}}$ have to be matricised to obtain a two-way data matrix [7,8,20]. This can be done in different ways, according to what one is interested in focusing on.

If the interest is on studying each sampling, a matrix $\mathbf{X}'_{\mathbf{b}}$ is obtained, having $I \times K$ rows and J columns. This approach is very straightforward in terms of computation, but since $I \times K$ is usually a rather large number, the interpretation of the resulting score plot can give some problems [21].

To focus on the objects, the data array $\underline{\mathbf{X}}$ can be matricised to $\mathbf{X}'_{\mathbf{a}}$ (I rows, $J \times K$ columns). The interpretability of the score plot is usually satisfactory but, when $J \times K$ is a large number, the interpretation of the loading plot may be very difficult. Similar considerations can be drawn when focusing on the sampling times: in this case, a matrix $\mathbf{X}'_{\mathbf{c}}$ is obtained (K rows, $I \times J$ columns).

Three-mode PCA allows a much easier interpretation of the information contained in the data set, since it directly takes into account its three-way structure. The final result is given by three sets of loadings together with a core array describing the relationship among them. If the number of components is the same for each way, the core array is a cube. Each of the three sets of loadings can be displayed and interpreted in the same way as a plot of standard PCA.

In the case of a cubic core array, a series of orthogonal rotations can be performed in the three spaces of the objects, variables and conditions, looking for the common orientation for which the core array is as much as possible body-diagonal [22]. If this condition is sufficiently achieved, then the rotated sets of loadings can also be interpreted jointly by overlapping them.

Trilinearity of the data set is also assumed, meaning that the effect of the objects is the same at any time and that the effect of time is the same for all the objects. Mathematically, it can be said that

$$x_{ijk} = \sum_{p=1}^{P}\sum_{q=1}^{Q}\sum_{r=1}^{R} a_{ip} b_{jq} c_{kr} g_{pqr} + e_{ijk}$$

where a_{ip}, b_{jq}, c_{kr} denote elements of the component matrices **A**, **B** and **C** of order $I \times P$, $J \times Q$, and $K \times R$, respectively, g_{pqr} denotes the elements (p, q, r) of the $P \times Q \times R$ core array $\underline{\mathbf{G}}$, e_{ijk} denotes the error term for element x_{ijk} and is an element of the $I \times J \times K$ array $\underline{\mathbf{E}}$.

A tutorial on chemical applications of multi-way analysis was presented by Henrion [23]. Kroonenberg [24] gave a detailed mathematical description of the model and discussed advanced issues such as data pretreatment/scaling and core rotation.

The data set was analysed by MATLAB routines (The Mathworks, Natick, MA, USA) developed by the authors and by the N-way toolbox by Bro [25].

2.6. Preprocessing methods

Preprocessing of higher-order arrays is more complicated than in the two-way case. The data set analysed in the present work had to be pretreated as to remove the systematic differences among the variables (due to the different scales and measurement units), preserving the differences related with sampling times (j-scaling). A different type of scaling (jk-scaling) removes the differences from the average trajectory. Depending on the preprocessing method applied, different models are obtained. In the following, a discussion is given about the effects of these two methods (j-scaling and jk-scaling) on the data structure for the final analysis.

In order to carry out j-scaling, the three way array $\underline{\mathbf{X}}$ is matricised to a two-way matrix $\mathbf{X}_{\mathbf{b}}$ having $I \times K$ rows and J columns. On it, a column autoscaling is performed; by doing that, the global variance of each variable is set to one and its mean value is set to zero, while the differences among the sampling times are preserved. jk-Scaling is obtained by matricising the original three-way array into a matrix having I rows and $J \times K$ columns, and then performing a column autoscaling (of course, in both cases, the two-way matrix is finally refolded onto the original three way array) [8].

3. Results and discussion

3.1. Analysis of colour

Samples were analysed using a UV-Visible spectrophotometer to determine the CIELab parameters during the wine ageing period.

The results showed that is only possible to register differences in colour characteristics between wines aged in contact with oak chips and wine aged in barrels after 400 days of starting wine ageing

Table 1
GC–MS results.

	2-Furaldehyde [μg L^{-1}]	Guaiacol [μg L^{-1}]	*cis*-Whiskeylactone [μg L^{-1}]	*trans*-Whiskeylactone [μg L^{-1}]	Eugenol [μg L^{-1}]
Sampling time T1 (30 days)					
Ca	186.3	52.3	81.4	60.7	5.8
Cf	296.4	62.3	19.0	79.9	8.0
Sa	1570.0	108.0	154.4	112.6	33.0
Sf	854.5	87.0	0.4	70.0	34.1
Ba	82.3	70.4	216.3	97.8	44.6
Bf	227.5	71.2	50.1	118.0	23.3
Sampling time T2 (90 days)					
Ca	462.4	72.6	96.6	85.2	9.2
Cf	619.5	72.1	80.3	126.7	13.3
Sa	1503.1	114.4	295.2	113.3	42.7
Sf	1492.3	114.1	0.8	37.7	37.7
Ba	503.3	79.6	332.4	138.3	72.2
Bf	762.4	76.1	129.6	219.8	31.1
Sampling time T3 (150 days)					
Ca	586.6	68.0	123.4	107.1	20.9
Cf	591.7	73.1	103.0	261.1	15.3
Sa	1458.5	128.5	249.5	155.8	57.8
Sf	1511.5	103.2	2.8	33.4	39.2
Ba	678.0	84.7	383.9	235.7	84.1
Bf	780.0	81.3	234.6	294.6	38.9
Sampling time T4 (330 days)					
Ca	188.2	53.7	248.2	161.8	50.2
Cf	199.6	43.8	240.16	341.2	34.0
Sa	902.7	61.7	399.1	30.1	93.2
Sf	844.3	73.4	20.4	106.2	63.3
Ba	580.8	42.2	697.6	184.3	92.1
Bf	424.4	38.4	354.2	228.7	66.6
Sampling time T5 (480 days)					
Ca	158.9	76.4	269.9	72.4	59.4
Cf	115.4	73.2	286.6	121.1	58.4
Sa	606.0	83.5	494.0	70.5	87.1
Sf	876.8	78.5	38.9	47.1	80.4
Ba	409.1	65.4	851.1	153.2	122.5
Bf	330.3	59.5	538.4	167.2	78.3
Sampling time T6 (600 days)					
Ca	77.2	116.2	282.3	60.1	76.4
Cf	97.0	119.8	321.1	96.9	74.9
Sa	885.1	73.7	498.3	73.7	84.9
Sf	771.6	69.9	76.6	14.0	43.2
Ba	264.3	80.2	907.5	127.1	129.7
Bf	208.2	73.7	564.0	143.4	94.8

Wines aged with alternative systems: Ca, American oak wood chips; Cf, French oak wood chips; Sa, American oak wood staves; Cf, French oak wood staves. Wines aged in traditional barrels: Ba, American oak wood barrel; Bf, French oak wood barrel.

process. This phenomenon could be explained in terms of chemical compounds associated with the pure red colour, such as anthocyanins [26], compounds that can easily react with acids, tannins, pyruvic acid and acetaldehyde, depending on the oxygenation level during ageing.

Usually, when wines are aged in barrels, an enhancement and stabilisation of the red colour may be due to condensation reactions. In this case, a natural and slow process occurs due to the oxygen constantly passing through the pores of the oak wood of the barrel walls. Instead, in the alternative ageing process, the oxygen was added in a single dose, established according to the average amount measured in the barrels [2]. In this way, molecules present in the alternative system were forced to react faster. Actually, several studies indicate that oak wood extract increases the loss of anthocyanins due to a higher degree of polymerisations [27].

The effects of this process were more evident when wine was aged in almost complete absence of oxygen during bottle maturation, because, in this phase, condensed and polymerised polyphenols have precipitated and the other compounds have continued reacting [28].

3.2. Gas chromatography

Table 1 shows the results of GC–MS analysis of five volatile compounds: 2-furaldehyde (F), guaiacol (G), eugenol (E), *cis*- and *trans*-whiskeylactone (CW, TW). The results showed the evolution of each compound during the maceration process for all type of wine ageing systems; e.g., the concentration of 2-furaldehyde significantly increased during barrel ageing and decreased during the period of bottle ageing, as it had already been reported [29]. Furthermore, the amount found in barrels was always higher than that measured in the case of alternative ageing techniques.

The decrease of 2-furaldehyde during bottle storage may be due to a slow chemical degradation or to a possible role as a precursor for the formation of other molecules linked to the furfuryl aldehyde functional group [30,31]. The results described here also indicated that furfural levels were similar during the first days of ageing process for all types of samples. However, the wines aged with chips showed a saturation point faster than wines aged in barrel, therefore the amount of furfural is always less for wines aged with chips during the period in bottle. These outcomes agree with the results reported by different authors [3,28,29].

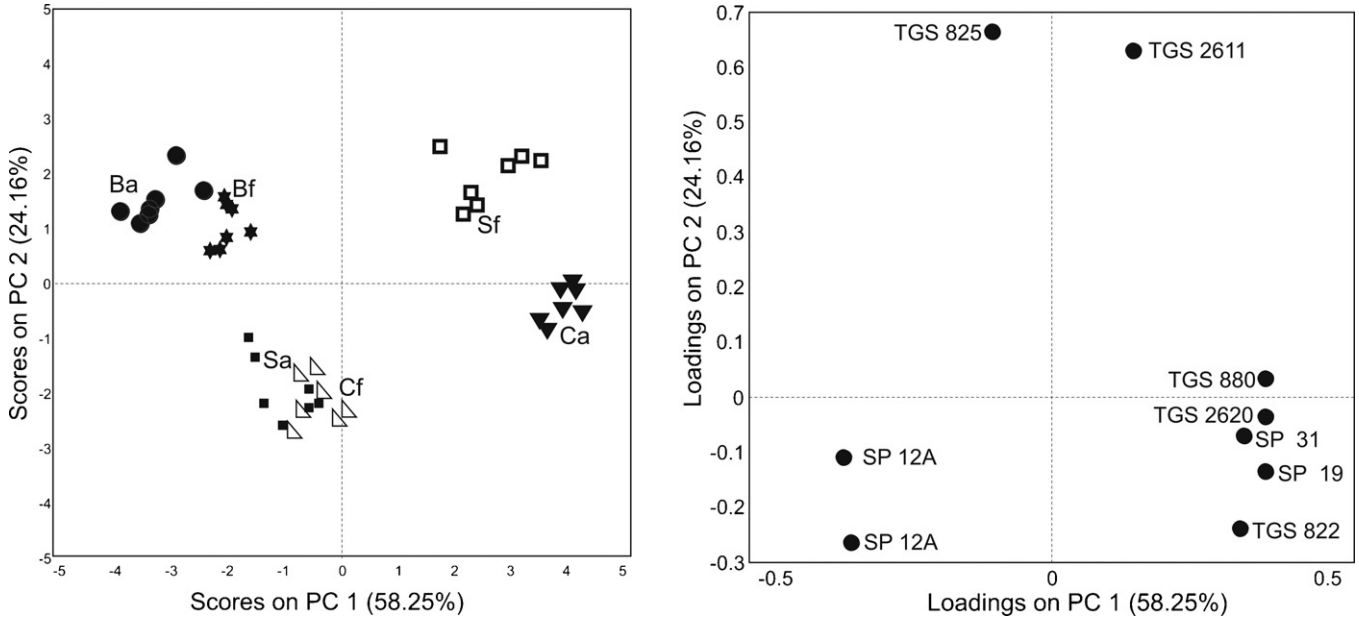

Fig. 2. PCA results of electronic nose (last sampling time). Dots, American barrel; stars, French barrel; filled squares, American staves; unfilled triangles, French chips; unfilled squares, French staves; filled triangles, American chips.

In all types of ageing a regular increase of *cis*-whiskeylactone concentration was observed up to day 600. The amount of this compound was always higher in wine aged in barrel. Several factors could explain this behaviour, one possibility being related to the stability of the aliphatic molecule of lactic acids and unsaturated fatty acids from whiskeylactone precursors [32]. Basically, this stability depends on the microbiological activity in presence of wood. A decrease of this activity, involving a degradation of oak lactones molecules, starts two years after the beginning of the wine ageing process [3].

Guaiacol, eugenol and *trans*-whiskeylactone also registered an increase during the first days of maturation (see Table 1). The trend followed by these volatile compounds showed that differences between types of ageing were more evident starting with bottle storage, with some compounds such as 2-furaldehyde decreasing, and other increasing, as for *cis*-whiskeylactone and eugenol. There were some considerable distinctions related to the wood origin. In case of guaiacol and eugenol, their quantities were higher for wine aged with American oak wood while for *trans*-whiskeylactone the highest level were found for French oak wood. Basically, this is due to complex condensation reactions and molecule degradations [33].

3.3. Electronic nose

The wines under study were exposed to the array of MOX sensors. The peak heights were used as input variables for data analysis and PCA was conducted on data from each sampling time. For shortness reasons, the results relative to just one period will be reported. Fig. 2 shows the scores and loadings plot of the two first principal components obtained on the autoscaled data of sampling time period 6 (PC1 = 58%, PC2 = 18% of total variance, respectively), where seven analytical replicates were performed on each sample. The wine aged in traditional barrels were located in a different position from the wine aged with alternative methods, but there was no systematic difference between staves and chips. It can also be seen that the analytical variability is smaller than the differences among samples.

3.4. Tucker3

In order to take into account the real data structure, a Tucker3 analysis has been applied on data arranged as a three-way array (wines × variables × sampling times). Both *j*-scaling and *jk*-scaling have been applied, since each pretreatment provides different and complementary information. To determine the correct dimensionality of the model, the routine Tucktest has been used [25].

Fig. 3 is the standard output of the Tucktest routine. It reports the complexity of the model (computed as sum of the components in the three modes) vs. the explained variance. The higher the complexity the higher the variance – and, consequently, the information – explained, but also the greater the difficulty in interpreting the results. Consequently, an optimal compromise has to be individuated. Fig. 3a shows that with *j*-scaled data the (1 2 2) model – explaining 69.8% of the total variance – represents the best compromise between explained variance and complexity. Fig. 3b shows the results of Tucktest on *jk*-scaled data, leading to the selection of the (2 2 2) model, explaining 46.1% of the total variance, significantly less than *j*-scaling, because the variability among sampling times has been removed. The core array for both preprocessings is reported in Table 2. In the core array for *jk*-scaling the superdiagonality has been maximised.

3.4.1. *j*-Scaled data

The interpretation of the results was based on the plot of the loadings combined with information in the core array elements. The model (1 2 2) indicated a single component for the first mode (objects) (Fig. 4a). Wines aged with chips (Ca and Cf) have the least

Table 2
Core array for Tuker3 model.

C_{111}	C_{121}	C_{112}	C_{122}
C_{211}	C_{221}	C_{212}	C_{222}
j-Scaling			
19.96	0.00	0.00	−9.52
jk-Scaling			
11.86	1.96	−3.00	2.43
−1.98	3.54	−2.46	−9.77

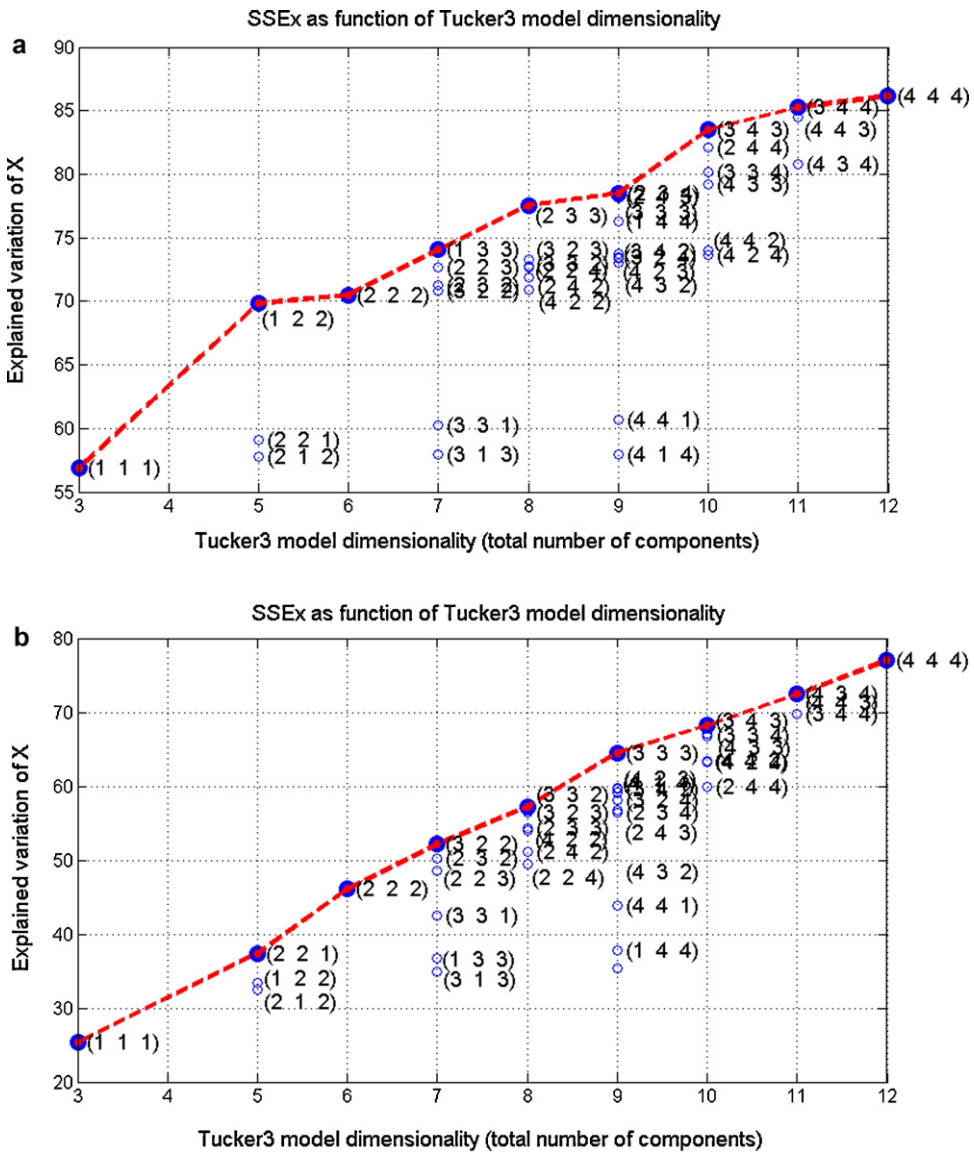

Fig. 3. (a) Explained variance vs. model dimensionality with *j*-scaled data. From the plot, the (1 2 2) model is easily detected as the best compromise between explained variance and complexity; (b) *jk*-scaled data. The (2 2 2) model is selected.

negative loading values, followed by wine aged with staves (Sa and Sf) and barrels (Ba and Bf), with very similar values. With this scaling the effect of the type of wine is very small, because *j*-scaling does not remove the effect of time, which is by far the largest source of variability. It is anyway interesting to notice the presence of a systematic effect related to the origin, with the loadings of the American samples (Ca, Sa and Ba) being consistently less negative than the corresponding French samples (Cf, Sf and Bf), especially for the staves and the barrels.

The loadings of the variables (see Table 3 for their coding) showed that the CIELab coordinates were grouped in one cluster with negative loadings on the first axis (Fig. 4b), this meaning that all these parameters bring similar information. As mentioned above, the coordinate S^* is inversely correlated to the other parameters. Consequently, its loading value is opposite to the whole set.

The variables of the electronic nose, except S_1, S_2 and S_7, have high loadings on the second axis, this meaning that their information is orthogonal to that brought by the CIELab coordinates.

Fig. 4c shows the scatter plot of the loadings of the third mode (conditions). Sampling times 1–3 (wine ageing process in barrel or tank) have positive loadings on the first axis, with progressively lower values on the second axis. This maturation process is mainly evident for condition 4 (sampling time of 330 days) which corresponds to the transition of wine from deposit to bottle. This behaviour can be explained by the fact that, in bottle, oxygen exposure is usually lower than during wine ageing in barrel, this changing the phenol structure of wines. Conditions 5 and 6 (bottle storage) are clearly differentiated by the rest of the conditions, showing negative loadings on the first axis.

The loadings of the conditions follow a well-defined V-shaped trajectory. By taking into account the loadings of the variables, it can be seen that in the conditions 1–3 (wine ageing in deposit or barrel), there is a progressive increase mainly of variables corresponding to sensors SP31 (S_8), SPMW1 (S_9) and TGS2620 (S_5), and a conforming decrease of other sensors such as SP12a (S_6), TGS2611 (S_4) and compounds such as guaiacol. This trend becomes very evident when going to condition 4 (the first sampling on bottled wine). After that, the trend previously observed reverses and, at the same time, there is an increase of variables corresponding to sensors TGS822 (S_1), TGS825 (S_2), SP19 (S_7), compounds such as *cis*-whiskeylactone

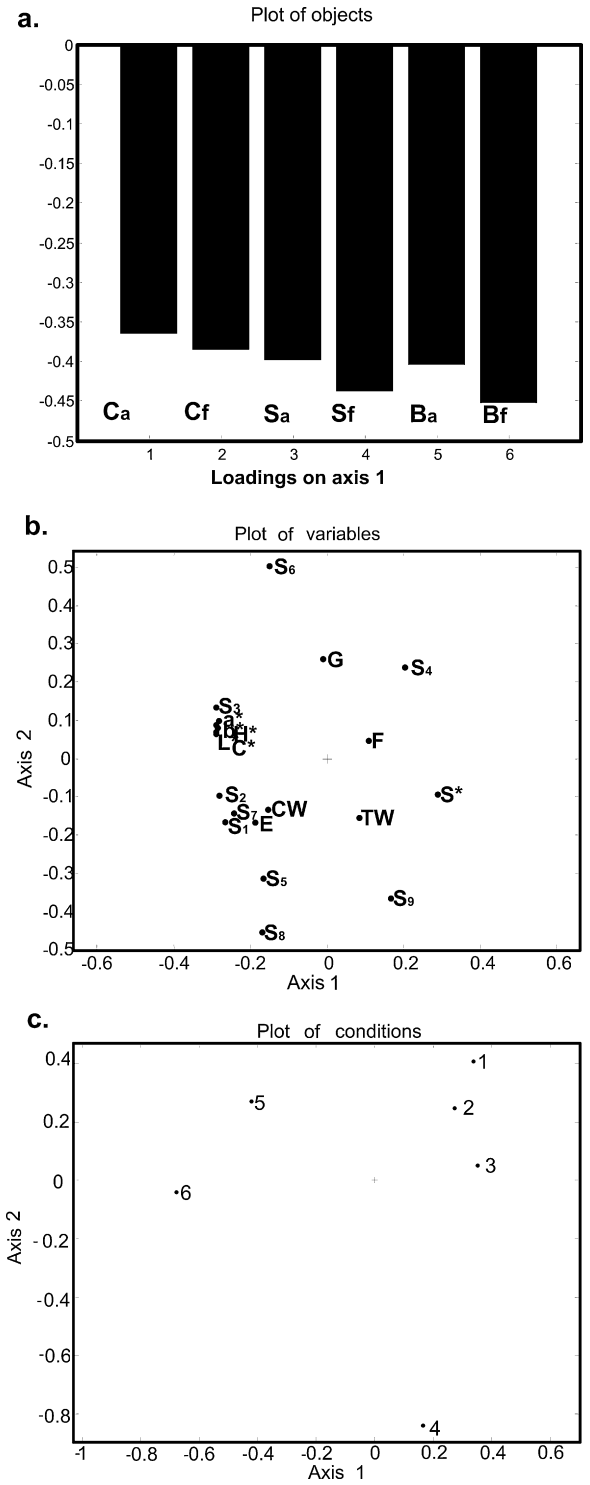

Fig. 4. (a) Bar plot of the loading of objects (*j*-scaled data). Wines Ca, Cf were ageing in alternative systems with chips, Sa, Sf with staves and Ba, Bf are wines ageing in barrels; (b) scatter plot of the loading of variables (*j*-scaled data) (see Table 2 for variable coding); (c) scatter plot of the loading of conditions (*j*-scaled data).

and eugenol and the CIELab variables, together with the decrease of coordinate S*. This behaviour may be a consequence of the reactions between colour-related compounds, as one of the effects of the microxigenation treatment.

Since the samples with French oak wood have more negative loadings on the first axis, it can also be said that variables S_1, S_2, S_7, *cis*-whiskeylactone and eugenol and the CIELab variables also

Table 3
List of variables evaluated.

Variable	Coding
UV–visible spectroscopy	
Lightness	L*
Position between red/magenta and green	a*
Position between yellow and blue	b*
Chroma	C*
Hue	H*
Saturation	S*
Gas chromatography	
2-Furaldehyde	F
Guaiacol	G
cis-Whiskeylactone	CW
trans-Whiskeylactone	TW
Eugenol	E
Electronic nose	
TGS822	S_1
TGS825	S_2
TGS880	S_3
TGS2611	S_4
TGS2620	S_5
SP12a	S_6
SP19	S_7
SP31	S_8
SPMW1	S_9

differentiate the origin of the samples. The gas sensors used in the e-nose were not selective towards individual compounds but appeared to have a general selectivity towards volatile compounds definitely related to wine ageing. Moreover, from the sensorial point of view, the correlation between the *cis-isomer* of whiskeylactone and sensors such as TGS822 (S_1), TGS825 (S_2) and SP19 (S_7) could be associated to fresh oak, coconut and vanilla odours. Wines with higher values of these compounds may exhibit more typical wood attributes [34]. Other reported compounds such as guaiacol, correlated with sensors TGS2611 (S_4) and SP12a (S_6), showed a minor influence in the sensory changes during the maturation process, which does not mean that they do not contribute to wine aroma. These types of volatile compounds may have additive or cumulative effects on the global composition.

3.4.2. *jk*-Scaled data

The loading plot of the *jk*-scaled data for the mode of the objects (Fig. 5a) shows a very clear effect of the treatment. As in the case for *j*-scaling, also *jk*-scaling shows a systematic effect related to the origin of oak wood used, with the greatest difference for wines aged with oak wood chips and the smallest for wines aged in barrels.

The plot of the loadings on the second mode (Fig. 5b) shows that the variables related to the electronic nose (S_1–S_9) and whiskeylactone (CW and TW) cluster at high positive loadings on the first axis. Eugenol (E), which is known to have an important impact on the aromatic characteristics of wine [35], has a highly positive loading on the first axis and a highly negative loading on the second axis. Guaiacol (G) and 2-furaldehyde (F), with negative loadings on the second axis, are positively correlated with S* and inversely correlated with the other CIELab variables.

Fig. 5c shows the scatter plot of the loadings of the *jk*-scaled data for the third mode, conditions. The pattern of the six sampling times is quite similar to what has been found for *j*-scaled data.

The high superdiagonality of the core matrix allows the joint interpretation of the three sets of loadings. Wines aged in barrels (Ba, Bf) have positive loadings on axis 1, this meaning that they have higher values of the e-nose variables, whiskeylactone (CW, TW) and eugenol (E). Since this effect is higher at the last samplings (conditions 5 and 6 are the ones with the highest loading on axis 1), it can be supposed that, at the end of wine ageing in barrel, the concentrations of these compounds are higher, suggesting that the

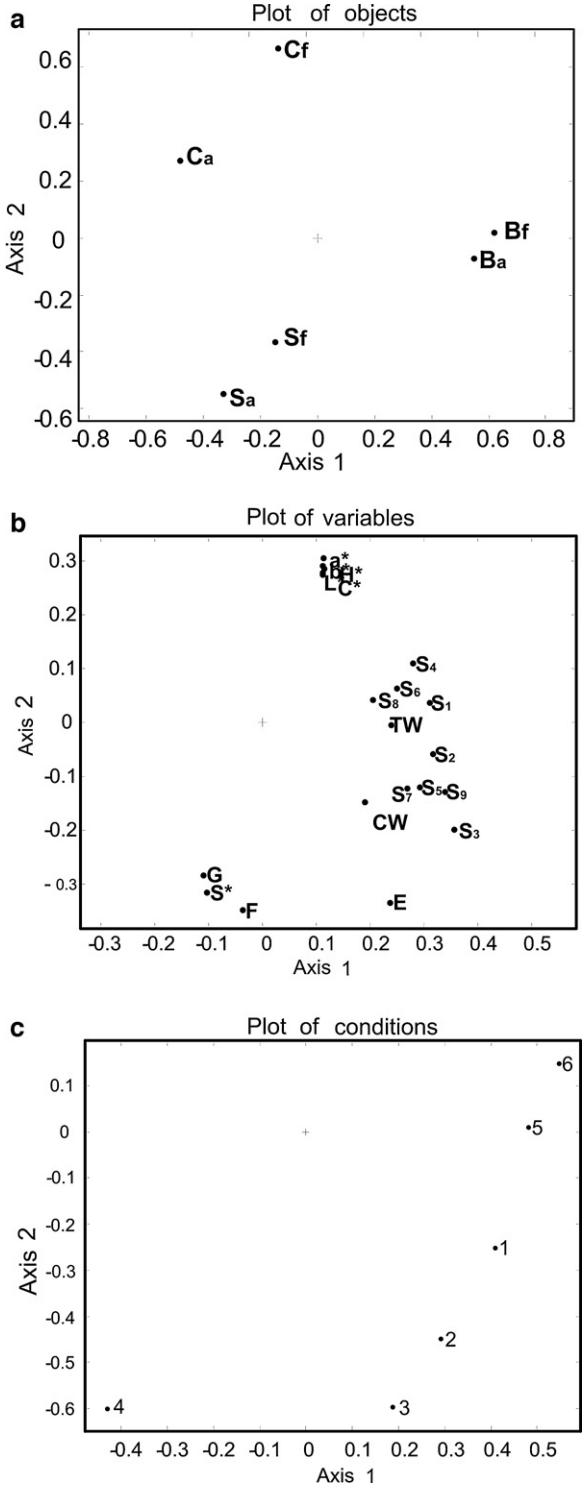

Fig. 5. (a) Scatter plot of the loading of objects (*jk*-scaled data). Wines Ca, Cf were ageing in alternative systems with chips, Sa, Sf with staves and Ba, Bf are wines ageing in barrels; (b) scatter plot of the loading of variables (*jk*-scaled data) (see Table 2 for variable coding); (c) scatter plot of the loading of conditions (*jk*-scaled data).

degradation of volatile compounds occurs earlier to wines aged in stainless steel tanks [33].

It was also possible to detect a systematic effect related to the origin of wood, because the samples macerated with American oak (Ca, Sa and Ba) showed higher values of variables 2-furaldehyde (F), guaiacol (G) and saturation coordinate (S*) and lower values of the CIELab coordinates than those aged with French oak (Cf, Sf and Bf), in good agreement with what has been found on the *j*-scaled data. These differences seem to be much greater in the samples aged with alternative systems than in the samples aged in barrels, and they are especially relevant at sampling time 4.

4. Conclusions

Tucker3 three-way analysis has been applied to the data generated by a sensor-based electronic nose, GC–MS and UV–visible spectroscopy, for monitoring winemaking processes. It has been shown that the multi-way method offers an interesting and valuable way to visualise the relationships between sensors responses and chemical composition of wines aged with different processes. In particular, it has been possible to highlight peculiar trends for different wine types, according to the ageing process or to the origin of the oak wood employed. The compounds that act as markers of such differences and descriptors of wine evolution have been identified. The present study was performed for exploratory purposes and, for this reason, a relatively low number of samples and sampling points over time were involved. Consequently, the conclusions drawn cannot be generalised. Anyway, based on the valuable results reported, upcoming studies are being designed involving more samples, in order to obtain deeper and broader comprehension of complex phenomena connected to wine ageing.

As for data processing, the results confirm that three-way analysis is more powerful than conventional PCA for the extraction of the maximum useful information from multidimensional data.

Acknowledgements

Financial supports from the Spanish Ministry of Science (Grant AGL2009-12660/ALI) and from the Italian Ministry of University and Research (PRIN 2008, CUP:D31J0000020001) are gratefully acknowledged. N. Prieto wishes to thanks for grant FPI from University of Valladolid.

References

[1] M.J. Cejudo-Bastante, I. Hermosin-Gutierrez, M.S. Perez-Coello, Food Chem. 124 (2011) 738–748.
[2] M. Del Álamo, I. Nevares, L. Gallego, B. Fernández de Simón, E. Cadahía, Anal. Chim. Acta 660 (2010) 92–101.
[3] I. Jarauta, J. Cacho, V. Ferreira, J. Agric. Food Chem. 53 (2005) 4166–4177.
[4] K.C. Persaud, P. Wareham, A.M. Pisanelli, E. Scorsone, Sensors Mater. 17 (2005) 355–364.
[5] G. Olafsdottir, P. Nesvadba, C. Di Natale, M. Careche, J. Oehlenschager, S.V. Tryggvadottir, R. Schubring, M. Kroeger, K. Heia, M. Esaiassen, A. Macagnano, B.A. Jorgensen, Trends Food Sci. Technol. 15 (2004) 86–93.
[6] J.W. Gardner, P.N. Bartlett, Electronic Noses: Principles and Applications, Oxford University Press, Oxford, 1999.
[7] A. Smilde, R. Bro, P. Geladi, Multiway Analysis, Applications in the Chemical Science, Wiley, England, 2004.
[8] R. Bro, Multi-way Analysis in the Food Industry, Models, Algorithms and Applications, Ph.D. Thesis, University of Amsterdam, 1998.
[9] R. Bro, C.A. Andersson, H.A.L. Kiers, J. Chemometr. 13 (1999) 295–309.
[10] F. Guimet, J. Ferré, R. Boqué, F. Rius, Anal. Chim. Acta 515 (2004) 75–85.
[11] G. Tomasi, J.H. Christensen, J. Chromatogr. A 1216 (2009) 7865–7872.
[12] T. Skov, R. Bro, Sens. Actuators B 106 (2005) 719–729.
[13] C. Cordella, R. Leardi, N.R. Douglas, Chemometr. Intell. Lab. Syst. 106 (2010) 125–130.
[14] M. Cocchi, C. Durante, M. Grandi, M. Manzini, A. Marchetti, Talanta 74 (2008) 547–554.
[15] C. Burian, J. Brezmes, M. Vinaixa, N. Canellas, E. Llobet, X. Vilanova, X. Correig, Sens. Actuators B 143 (2010) 759–768.
[16] Office International de la Vigne et du Vin (OIV), Recueil des méthodes internationales d'analyse des vins et des moûts, Paris, 1990, pp. 41–58.
[17] J.D. Carrillo, A. Garrido-López, M.T. Tena, J. Chromatogr. A 1102 (2006) 25–36.
[18] M.L. Rodriguez-Mendez, A.A. Arrieta, V. Parra, A. Bernal, A. Vegas, S. Villanueva, R. Gutierrez-Osuna, J.A. de Saja, IEEE Sens. J. 4 (2004) 348–354.
[19] S. Villanueva, A. Guadarrama, M.L. Rodriguez-Mendez, J.A. de Saja, Sens. Actuators B 132 (2008) 125–133.

[20] D.L. Massart, B.G.M. Vandeginste, S.N. Deming, Y. Michotte, L. Kaufman, Chemometrics: A Textbook, Elsevier, Amsterdam, 1998.
[21] R. Leardi, C. Armanino, S. Lanteri, L. Alberotanza, J. Chemometr. 14 (2000) 187–195.
[22] R. Henrion, J. Chemometr. 6 (1993) 477–494.
[23] R. Henrion, Chemometr. Intell. Lab. Syst. 25 (1994) 1–23.
[24] P.M. Kroonenberg, Three-Mode Principal Component Analysis: Theory and Applications, DSWO Press, Leiden, 1983.
[25] C.A. Andersson, R. Bro, Chemometr. Intell. Lab. Syst. 52 (2000) 1–4.
[26] M.C. Llaudy, S. Roser Canals, M. Gonza Lez, J.M. Canals, C. Santos-Buelga, F. Zamora, J. Agric. Food Chem. 54 (2006) 4246–4252.
[27] J. Wirth, C. Morel-Salmi, J.M. Souquet, J.B. Dieval, O. Aagaard, H. Vidal, H. Fulcrand, V. Cheynier, Food Chem. 123 (2010) 107–116.
[28] V.L. Singleton, Am. J. Enol. Viticult. 38 (1987) 69–77.
[29] J.J. Rodríguez-Bencomo, M. Ortega-Heras, S. Pérez-Magariño, C. González-Huerta, J. Agric. Food Chem. 57 (2009) 6283–6391.
[30] P.J. Spillman, A.P. Pollnitz, D. Liacopoulos, K.H. Pardon, J. Agric. Food Chem. 46 (1998) 657–663.
[31] J.L. Perez-Prieto, J.M. Lopez-Roca, A. Martinez-Cutillas, F. Pardo-Minguez, E. Gomez-Plaza, J. Agric. Food Chem. 51 (2003) 5444–5449.
[32] P. Chatonnet, J.N. Boidron, Sci. Aliments 8 (1988) 479–488.
[33] K.L. Wilkinson, G.M. Elsey, R.H. Prager, A.P. Pollnitz, M.A. Sefton, J. Agric. Food Chem. 52 (2004) 4213–4218.
[34] N. Loscos, P. Hernandez-Orte, J. Cacho, V. Ferreira, Food Chem. 120 (2010) 205–216.
[35] P. Arapitsas, A. Antonopoulos, E. Stefanou, V.G. Dourtoglou, Food Chem. 86 (2004) 563–570.